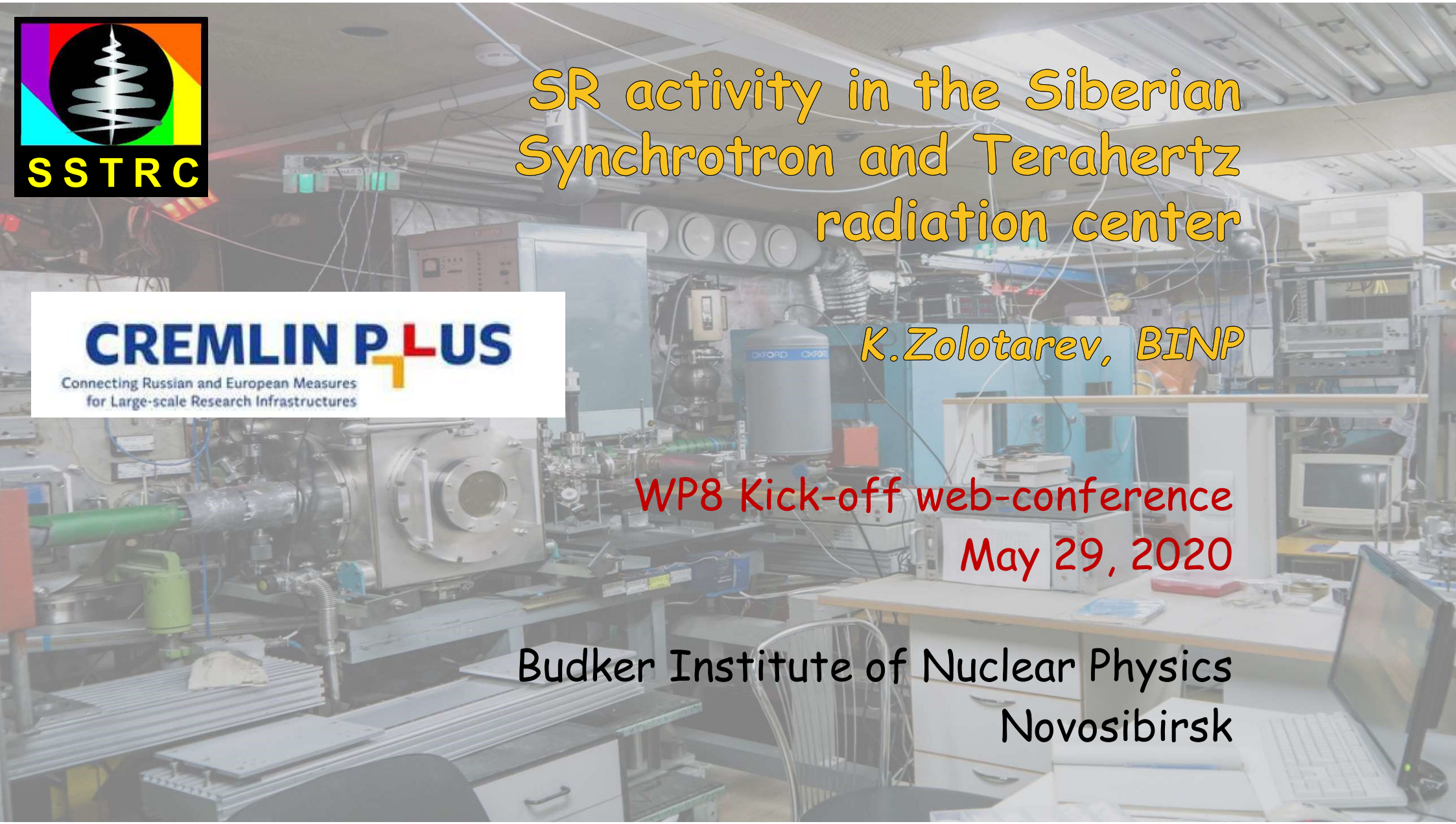

SR activity in the Siberian Synchrotron and Terahertz radiation center

K.Zolotarev, BINP

WP8 Kick-off web-conference
May 29, 2020

Budker Institute of Nuclear Physics
Novosibirsk

SSTRC History

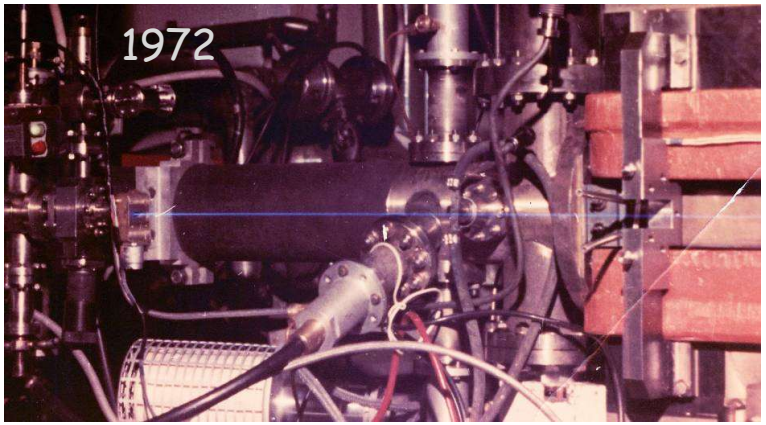

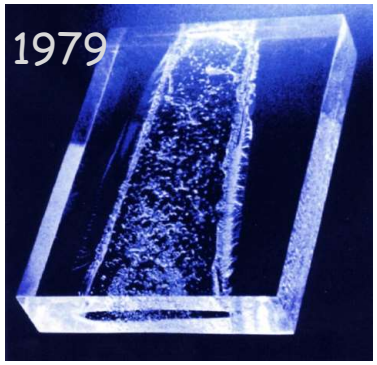

Light source in the Novosibirsk

- Optimal geographical location
- Unique interdisciplinary scientific infrastructure
- Big number of the regional universities with broad profiles
- Experienced users society from Siberian center of synchrotron and terahertz radiation (collective resources center)
- International cooperation with Kazakhstan. Mongolia. China

User potential

- **About 50 institutes of the Siberian and Ural Branches Russian academy of science**
- **About 10 universities from Novosibirsk. Tomsk. Krasnoyarsk. Irkutsk . Ekaterinburg and other**
- **A number of the industrial enterprises from Siberian region**

SSTRC
Main directions

- SR applications activity
- FEL developing, building, maintenance and upgrading
- FEL radiation applications in the teraherz rage
- Developing and fabrication superconducting insertion devices
- Developing and fabrication magnetic elements for accelerators
- Developing of the new light source for SSTRC
- SR and FEL conferences organization
- Education activity
- International collaborations

BINP superconducting ID over the world

SFR-2020

Synchrotron and Free electron laser Radiation: generation and application (SFR-2020)

13-16 July 2020
Budker INP

https://indico.inp.nsk.su/event/24/

WEB site of the SSTRC - https://ssrc.biouml.org/#!

Light sources in the SSRTC

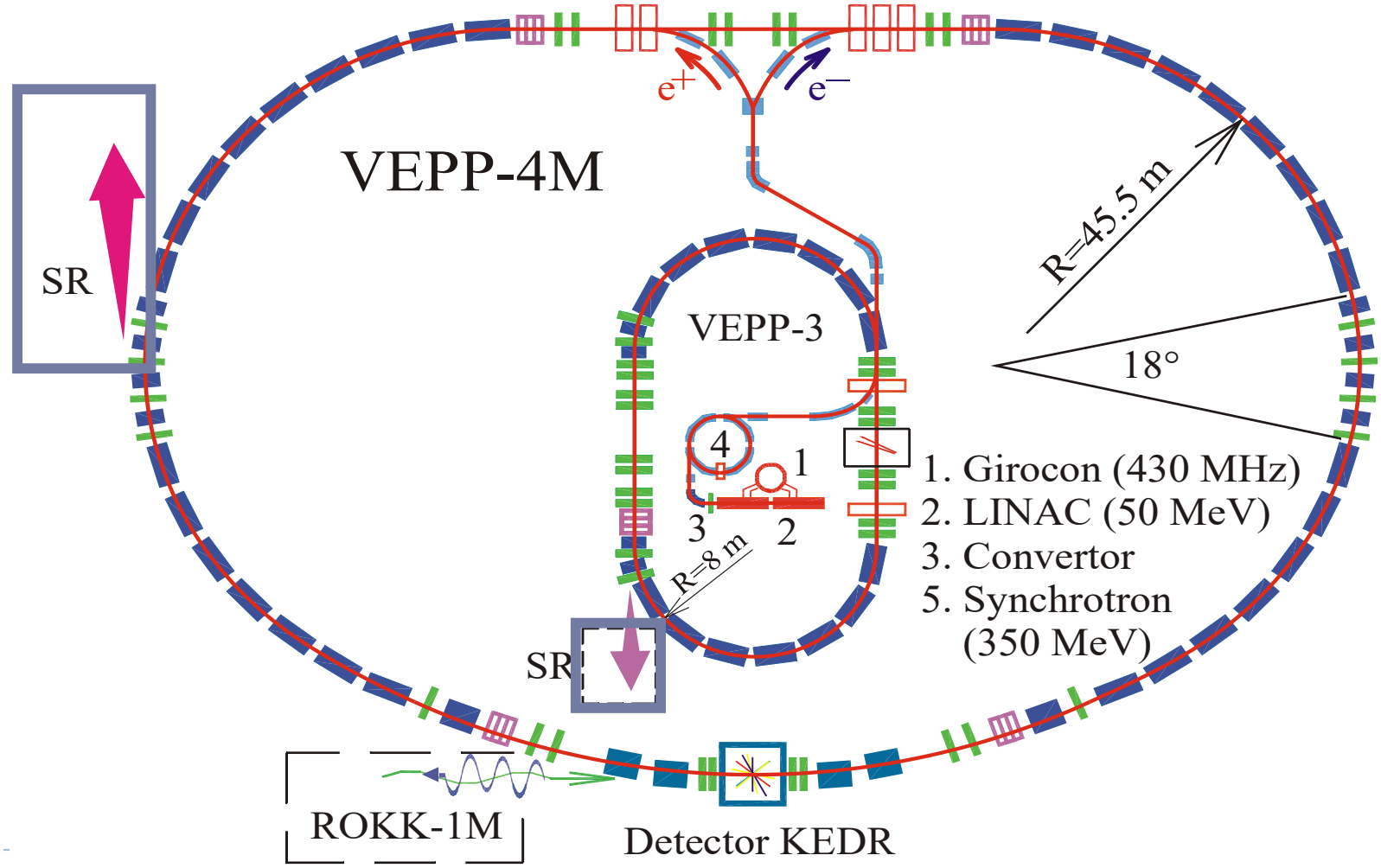

SR sources

	VEPP-3	VEPP-4M Low Energy	VEPP-4M High Energy
Energy, GeV	2	1.8	4.5
Circumference, m	72	366	
Lattice type	FODO	FODO	
Emittance, nm rad	~300	25	120
Max. current, mA	100	20	20
Number of bunches	1 - 2	1, 2, 4, 8	1, 2, 4, 8
SR devises	Wave length shifter (2 T)	Bending magnet (0.38 T)	Multipole wiggler (1.3 T x 5 poles)
Optic function in irradiation point β_x, β_y, η_x, m	2, 4.5, 0.7	9.64, 7.9, 0.9	9.7, 7.9, 1.16
Source size in irradiation point $\sigma_x \times \sigma_y$, mm	0.9 x 0.3	2.3 x 0.1	1.5 x 0.25
Critical energy, keV	5.3	0.8	13.8
Number of beamlines	8	1	1 (3 stations)

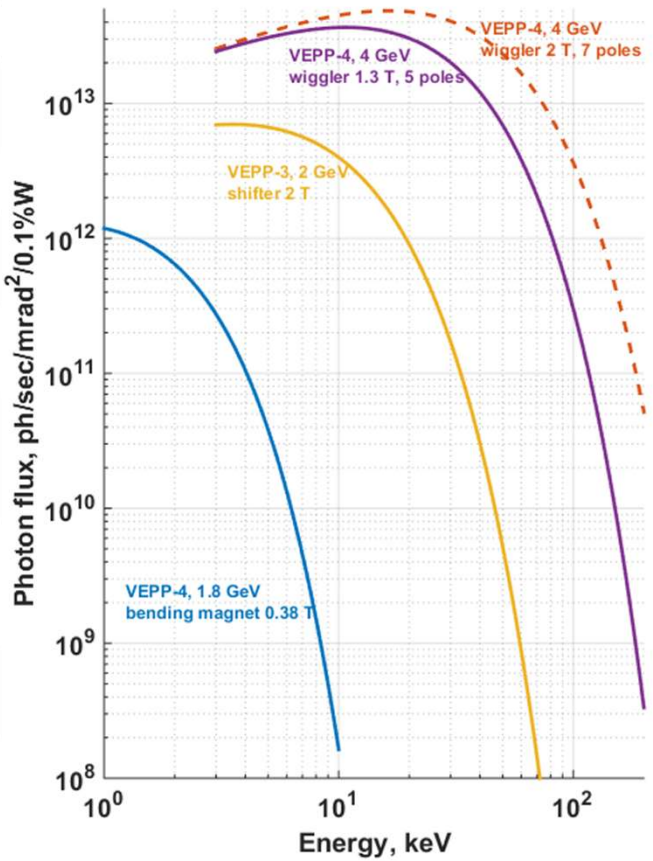

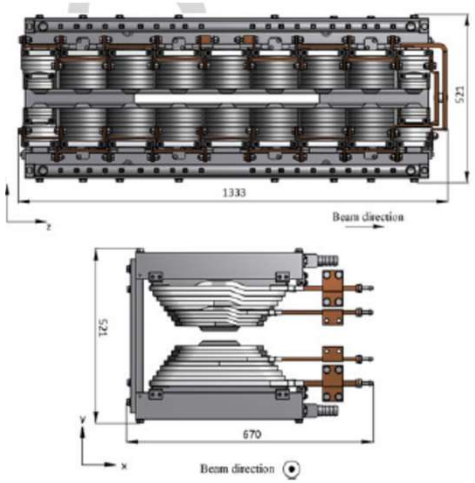

Hybrid EM/PM wiggler (VEPP-4M)

7 + 2 poles

B_0 = 2 T

λ_u = 140 mm

VEPP-3 synchrotron radiation beamlines

VEPP-3 SR experimental hall (14x5 m)

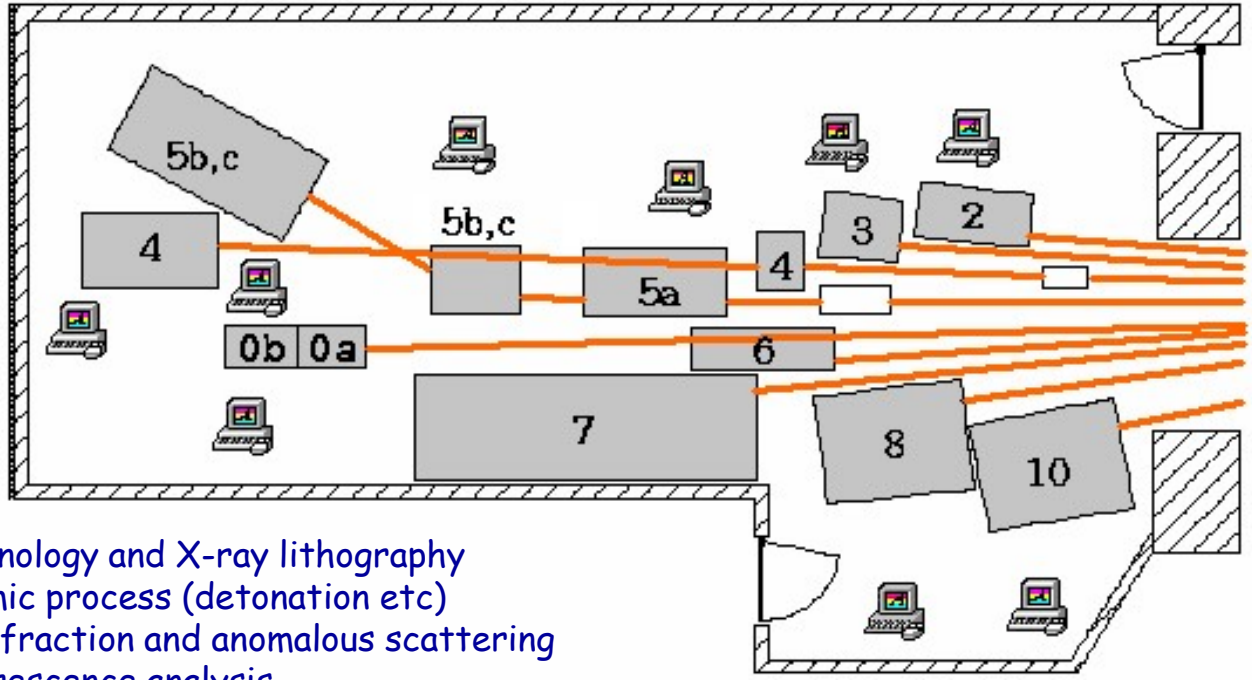

0a - LIGA-technology and X-ray lithography
0b - Fast dynamic process (detonation etc)
2 - Precise diffraction and anomalous scattering
3 - X-ray fluorescence analysis
4 - High pressure diffraction
5a – X-ray microscopy and microtomography
5b – Time resolved diffraction
5c – Small angle scattering
6a - Time resolved luminescence
6b – Precise diffraction-2
7 - SR monitoring station
8 - EXAFS-spectroscopy

VEPP-4 SR beamlines

1. «Cosmos» (metrology in VUV and soft X-ray range 10-2000 eV)
2. Phase contrast microscopy, microtomography and hard X-ray fluorescence
3. XRF in hard X-ray range
4. «Vzryv-2» (nanosecond diagnostics)
5. "Plamya" beamline
6. Precise difractometry

X-ray Lithography and LIGA-technology

Single microbeam SR or microbeams array are used for Direct X-ray lithography for Fabrication of deep LIGA structures.

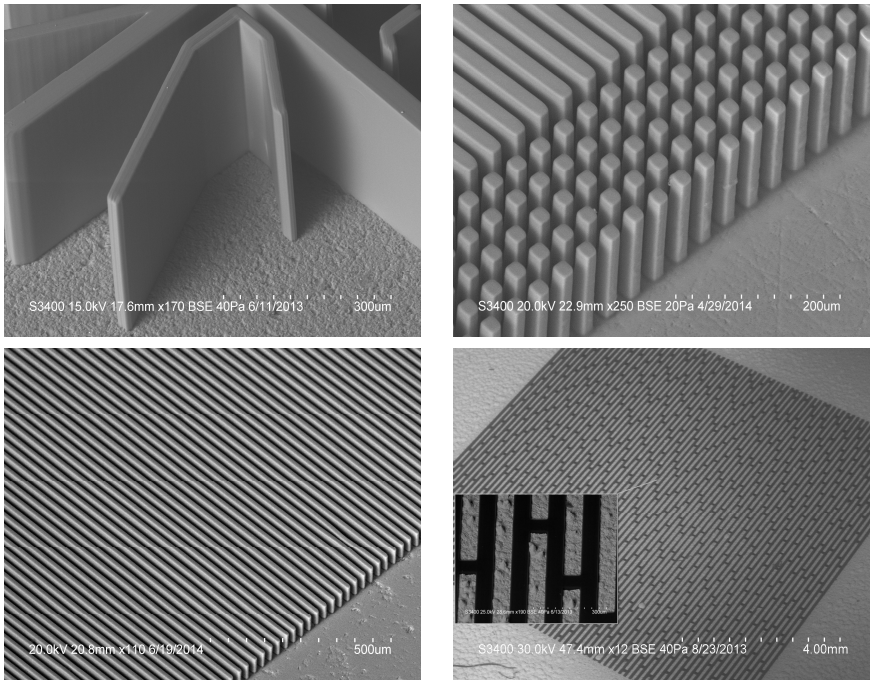

Samples of high aspect ratio microstructures: micro-lamellae, micro-grid, array columns

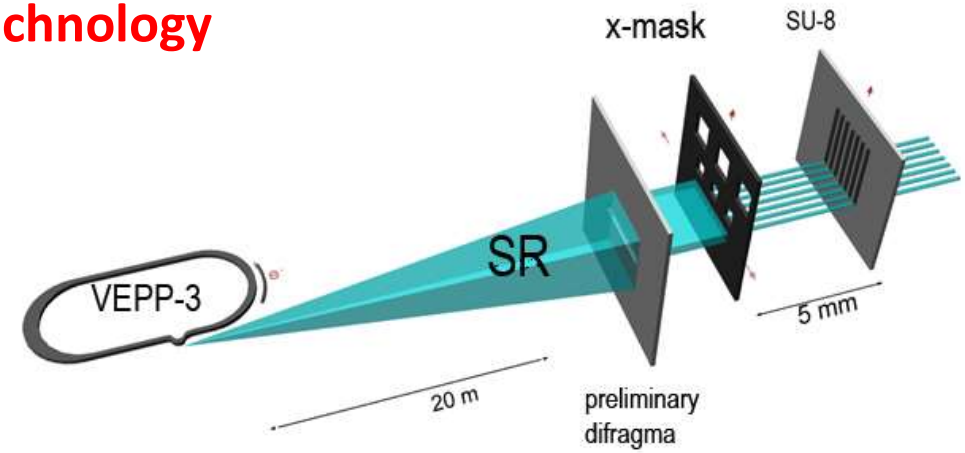

Electron lithography.
SEM Hitachi Type II + Nanomaker for microstructure forming in the thin PMMA layers (2-3 μm) for fabricating intermediate template for the soft X-ray lithography

Scanning μSRXRF
Confocal polycapillary X-ray optics

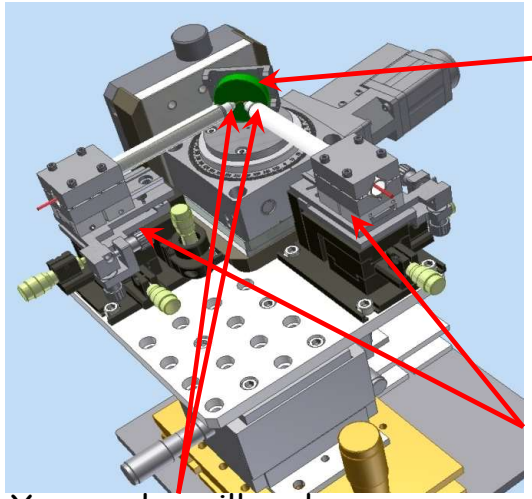

X-ray polycapillary lenses

Lenses adjustment stages

Microfluid insertions

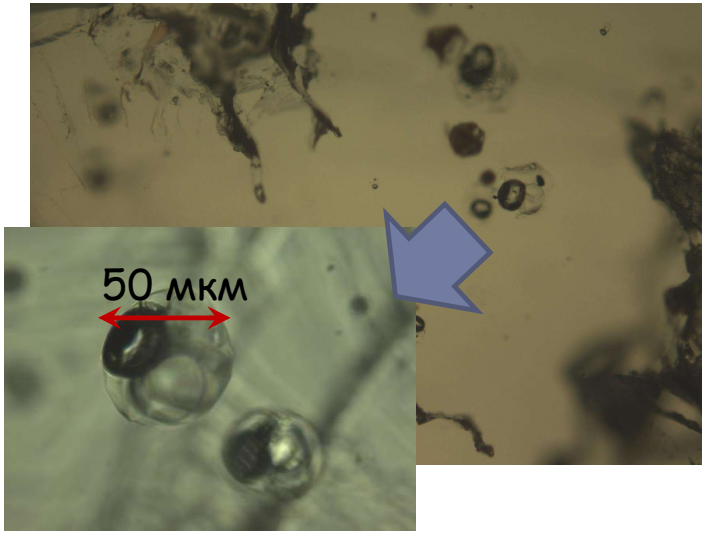

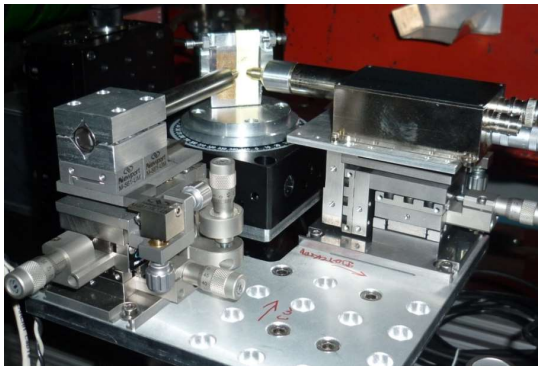

Spatial resolution about 10 μm
3d reconstruction

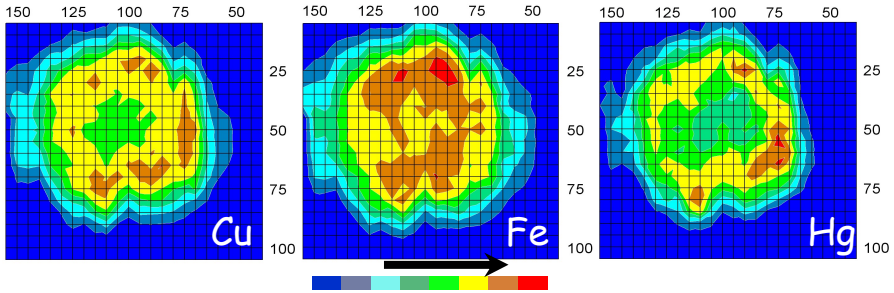

Elements distribution in the coss-section of the human hair

Equipment for XRD experiments with high pressure and high temperatute
Beamline 4, VEPP-3

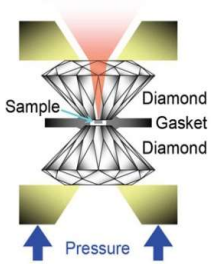

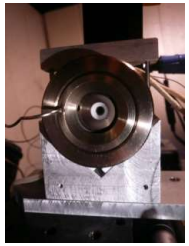

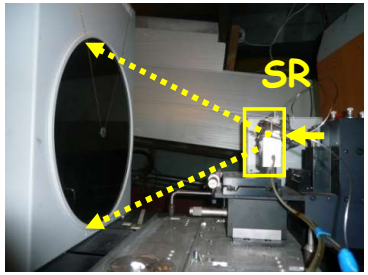

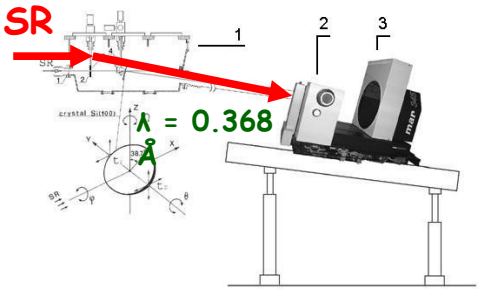

High pressure diamond anvil cell and general view for the diffraction experiment

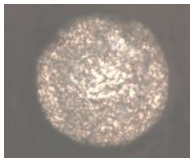

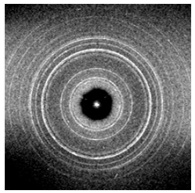

View in the chamber and the paten of powder sample at P ≈ 3 GPa

Stability of hydrocarbon compounds at high pressures and temperatures and implications for the deep structure of the Earth and planets

polycyclic aromatic hydrocarbons - important components of inclusions in the deep minerals and meteorites

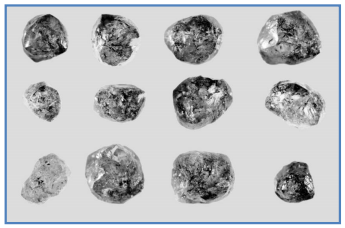

polyphase inclusions hydrocarbons in diamonds from deposits north-east Siberian platform (Томиленко и др., 2001, Доклады РАН).

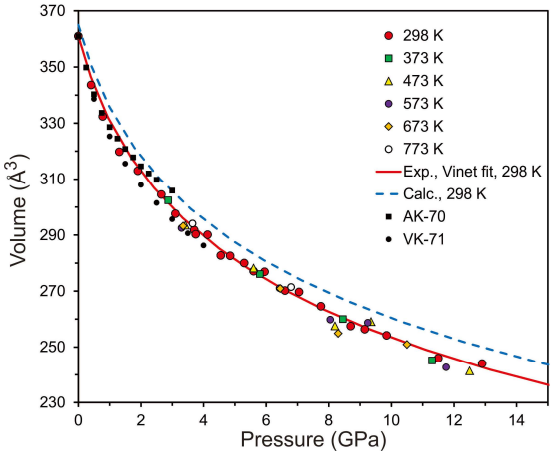

Pressure dependence of the unit cell volume of naphthalene $C_{10}H_8$ at 298-773 K.

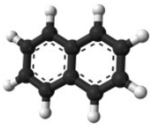

molecule naphthalene

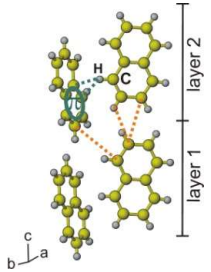

Structure and anisotropic compressibility naphthalene 0-6 GPa

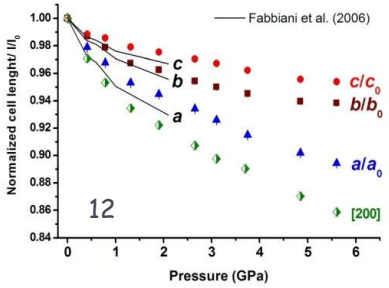

Murchison meteorite
Aromatic hydrocarbons predominate in hydrocarbon matter of meteorites(*Pering, 1971, Science*

X-ray microscopy and microtomograpy

Main layout

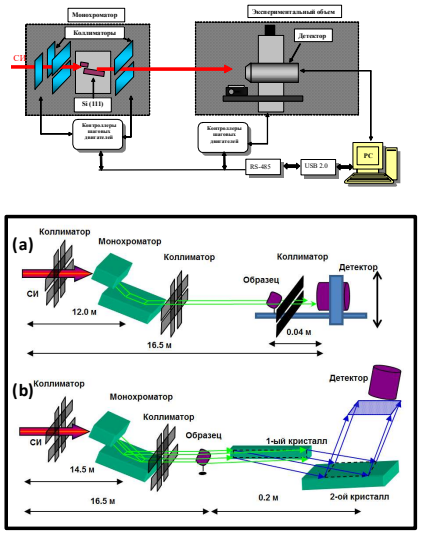

Imaging schemes
(a) - without magnificationt, (b) - scheme using asymmetrically cut crystals

The main parameters of the station
Monochromator:
Two crystals, silicon, (+ n, -n) c working crystallographic plane (111)
The range of photon energies of monochromatic radiation: 5-45 keV
Spatial resolution
In the circuit without increasing: 50 μm
In the circuit with increasing 2 μm

Monochromator

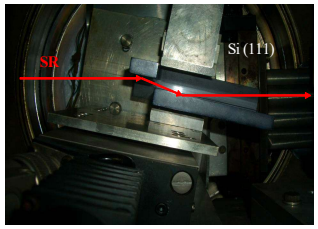

Channel cut monochromator: Si (111)

Experimental hatch

1 - sample 2 - first asymmetrical crystal, 3 - second asymmetric crystal, 4 - Detector

Two dimensions detector"Photonic Science"

Effective range: 62 x 41 mm2
The scintillator: Gadolinium oxysulfide
Energy range: optimum 5 - 35 keV
Range of registration: 65536 (16-bit)

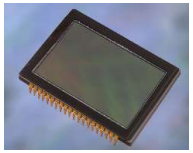

CCD 4008 x 2670
pixel size 9x9 μm²

Fiber optics with magnification 1.73

Testing of the X-ray transparent coatings

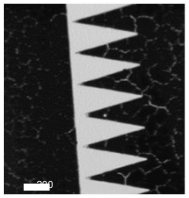

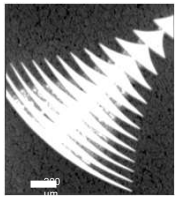

Density distribution in the explosive

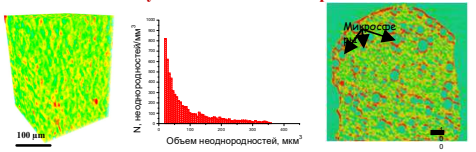

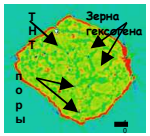

TNT and hexogen mixture

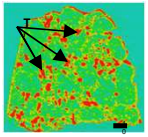

Hexogen with 7% Tl_n

Minerals distribution in geological samples

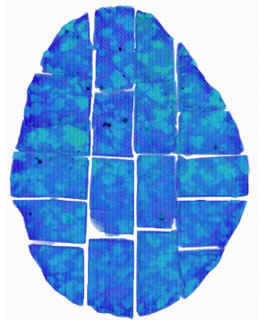

X-ray topography on natural diamonds

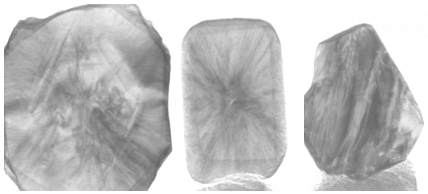

Archaeological research

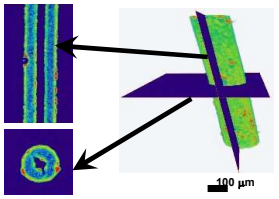

Hair from accent barrows

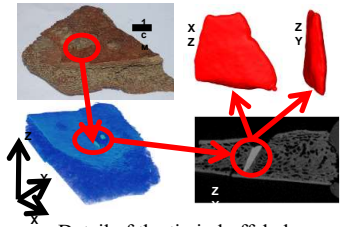

Detail of the tip in buffalo bones

Precise diffractometry

General view

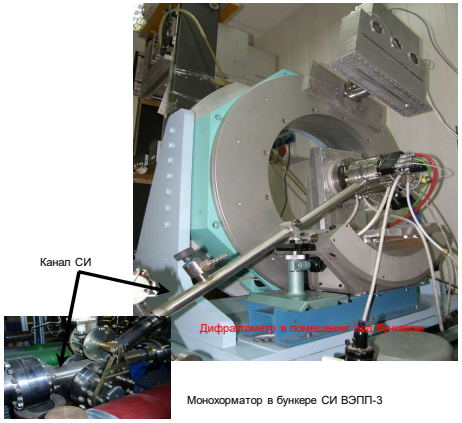

Layout

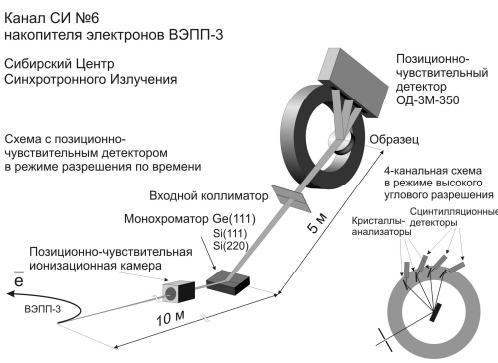

The main parameters of the station
Monochromator:
A single-crystal, with the beam deflection in the vertical plane at an angle ofapproximately 30 °;
Crystals: Ge (111), Si (111), Si (220);
The discrete set-energy radiation:
7.162 keV, 7.460 keV, and 12,183 keV
collimator:
Slits output;
beam on the sample size 0.5 × 5 mm2
detection systems:
One-coordinate detector OD-3M-350;
The range of angles 30 °, resolution 0.01 °, the time resolution of 1 ms.
Sample Holders:
High-temperature X-ray cameras Anton Paar XRK-900 and HTK-2000

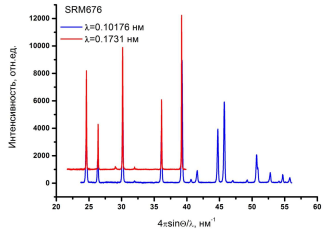

XRD patterns of corundum, obtained at different photon energies in a fixed detector position

Realized methods

diffractometry with time resolution at high temperatures (up to 1400 ° C in air to 2000 ° C in vacuum);
diffractometry with time resolution in a reaction medium (up to 900 ° C at gas pressures from 0.1 mbar to 10 bar);

Equpment

High temperature X-ray chambers

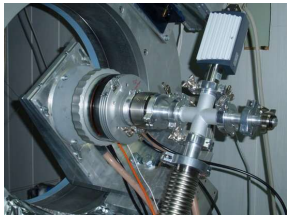

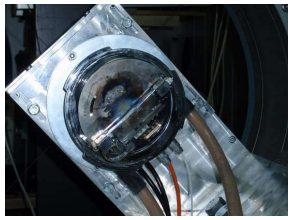

Luggage Anton Paar HTK-2000 experiments at temperatures up to 1400 ° C in air or an inert atmosphere to 2000 ° C in vacuum.

Camera Anton Paar XRK-900 experiments at temperatures up to 900 ° C in an oxidizing or reducing environment, and gas mixture pressure of from 0.1 mbar to 10 bar

- 3-channel system of preparation of gas mixtures on the basis of mass flow-controllers;
- hydrogen generator
- Gas analyzer based on SRS RGA-100 quadrupole mass spectrometer

Corundum lattice parameter change due to thermal expansion by heating in an inert atmosphere. Camera XRK-900, envinment - He.

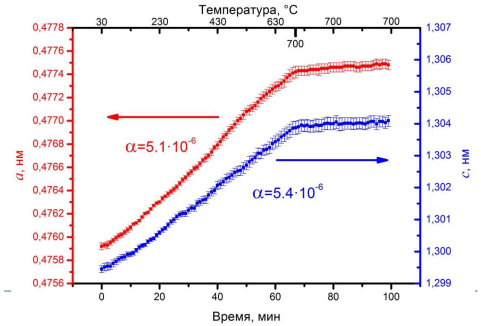

Phase composition of Ni-Cu catalysts for the synthesis of nitrogen-containing carbon nanofibers and its changes in response

Changing the state of the catalyst in a reaction medium. 100% C2H4

Changes in the catalyst lattice parameter in a reaction medium. 100% C2H4

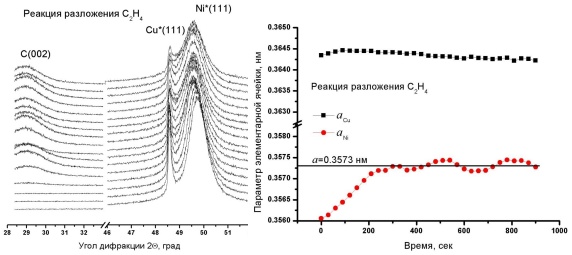

Autooscillations reaction rate in the catalytic oxidation of light hydrocarbons to Ni and Pd

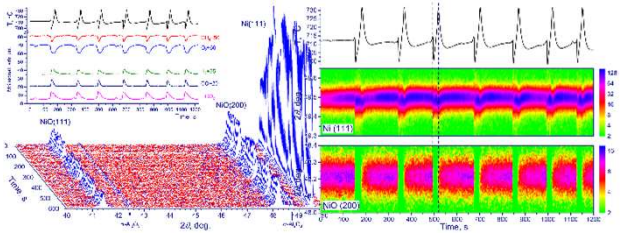

In Situ Investigation of the structure changes alloy based on zirconium with saturated hydrogen from the gas phase

XAFS

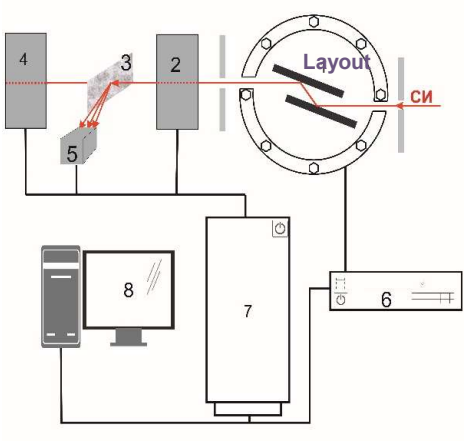

1 - two-crystal monochromator; 2.4 - ionization chambers; 3 - the sample; 5 - the detector (PMT / PDP); 6 - the controller; 7 - management and recording system; 8 - PC

It was found that the structure of the shell of the active component Pd-Au catalysts, leading to high process selectivity.

General view

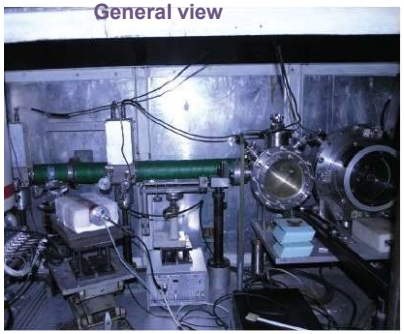

Research applied Pd-Au catalyst raw material processing systems from renewable resources for pharmacology and medicine

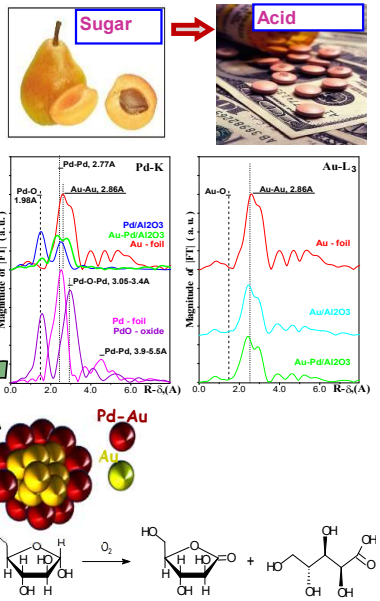

Purposes

Carrying XANES and EXAFS researches - determination the charge states of the elements and structure of the local agents in various states of aggregation.

Main parameters

Monochromator: channel cut, silicon, crystallographic planes (111).
The range of photon energies of monochromatic radiation: 5-32 keV
The concentration of the studied element 0.01-100%.
Possibility of measurements techniques - transmittance and fluorescence output (in current and counting modes).

*** A study of catalytic nano and precursors for various processes.**
*** A study of functional nanomaterials, nano-semiconductor, thin nanostructured films.**
*** Study of organometallic compounds compounds and inorganic complex composition.**
*** The study of biological objects and archaeological finds.**

Study of CVD films of hf and Al oxides

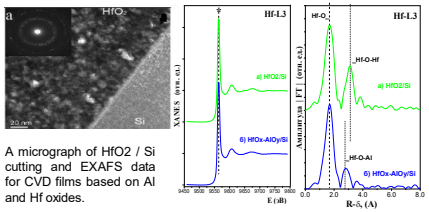

A micrograph of HfO2 / Si cutting and EXAFS data for CVD films based on Al and Hf oxides.

It was established that the method of CVD beta-diketonate complexes Hf and Al nanocrystalline film obtained solid solutions of mixed oxides.

X-ray detectors “Scionix” and “Canberra”

A study of low-interest Ni-Au catalysts for the conversion of biomass fermentation products for alternative energy

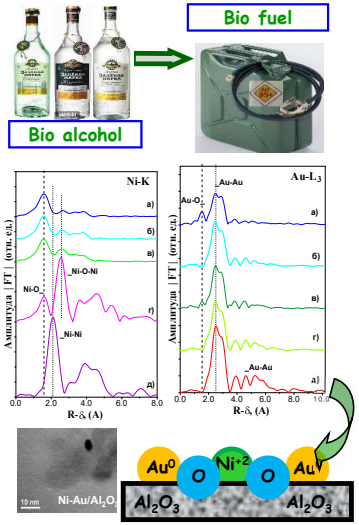

It is shown that the active catalyst Ni-Au component has features of the structure causing high catalytic activity.

New stations on the wiggler beamline from VEPP-4 storage ring

Phase contrast microscopy

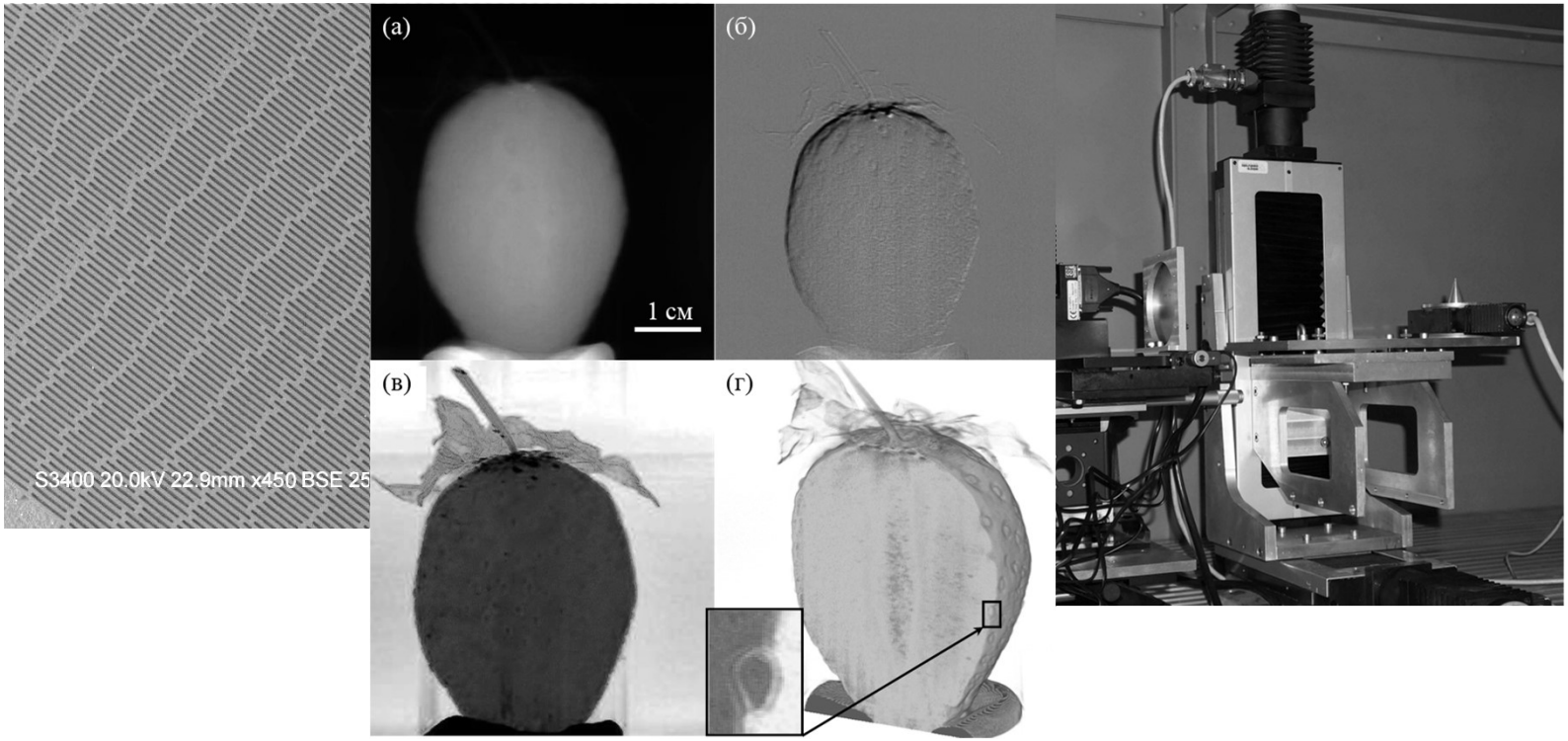

(а) – Absorption contrast, (б) – Differential phase contrast ∂Φ(x)/∂x, (в) – phase contrast Φ(x), (г) – Tomographic reconstruction of three-dimensional structure of strawberries set phase projections.

X-ray data of the crystallization sequence became AISI 304 with high time resolution

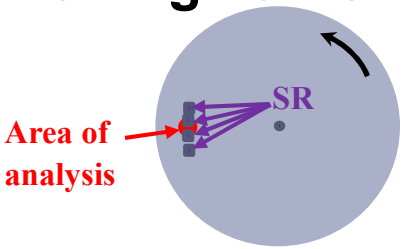

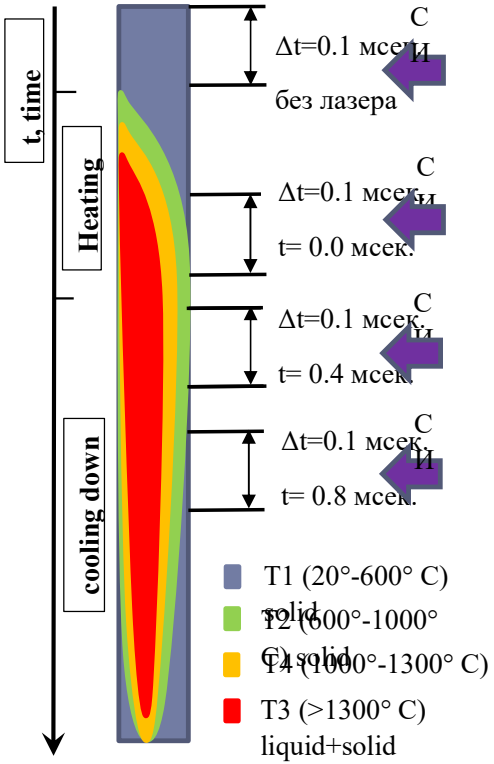

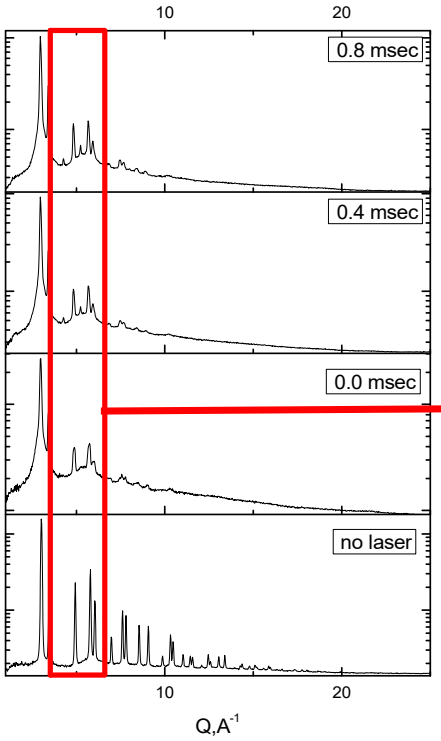

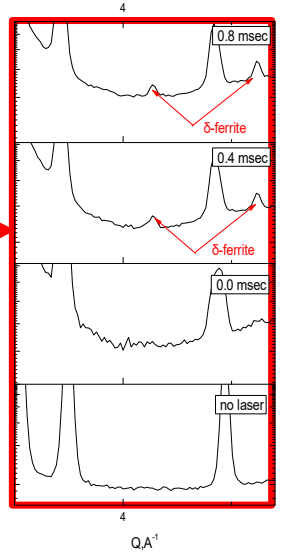

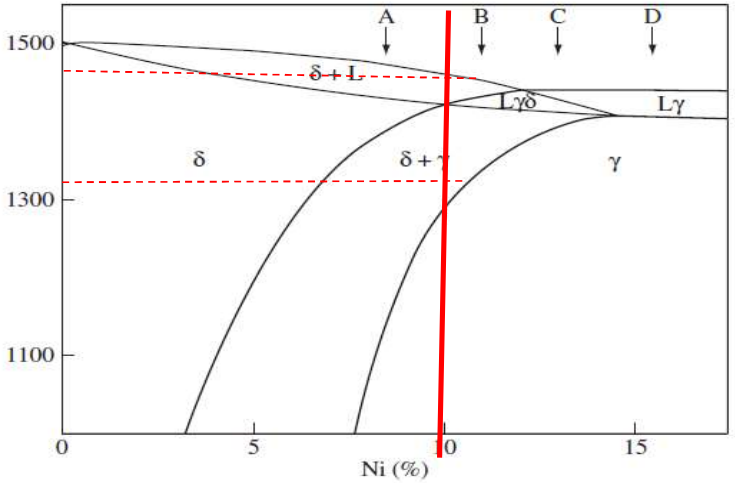

Figure 1. Temperature (°C) vs. nickel content (in wt. (%)). Section through Fe-Ni-Cr phase diagram at 19 wt. (%) Cr showing four solidification modes[3].

Studies of the effectiveness of radiation therapy in hypoxia conditions caused by manganese nanoparticles.

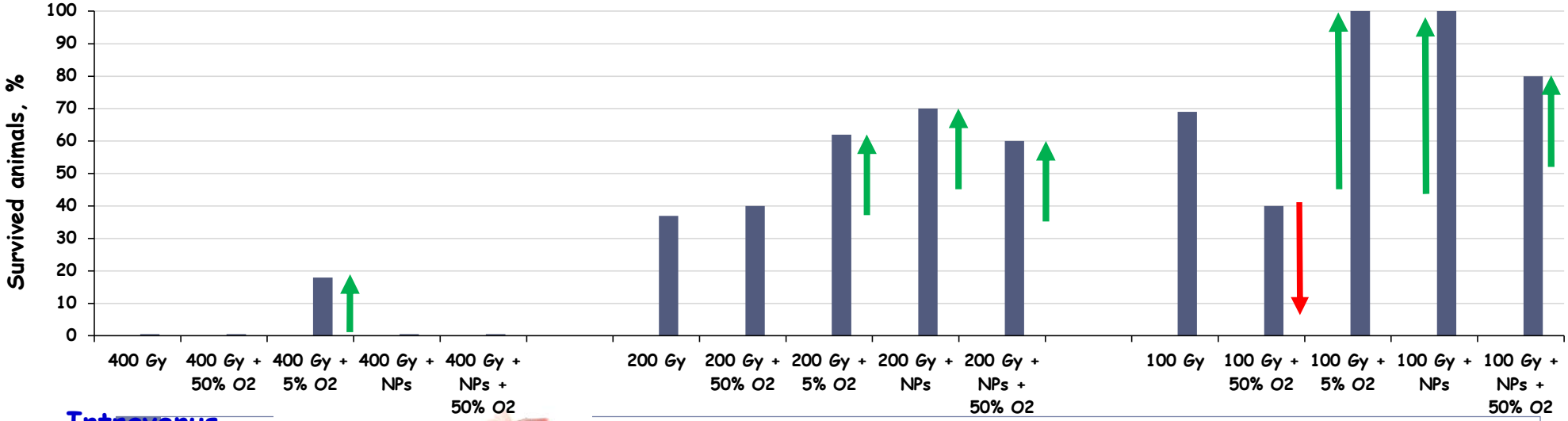

Intravenus
MnO 45 mg/kg

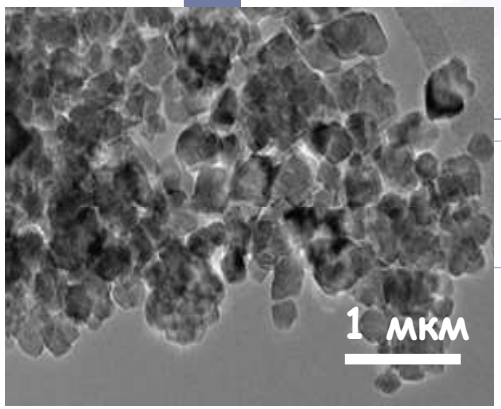

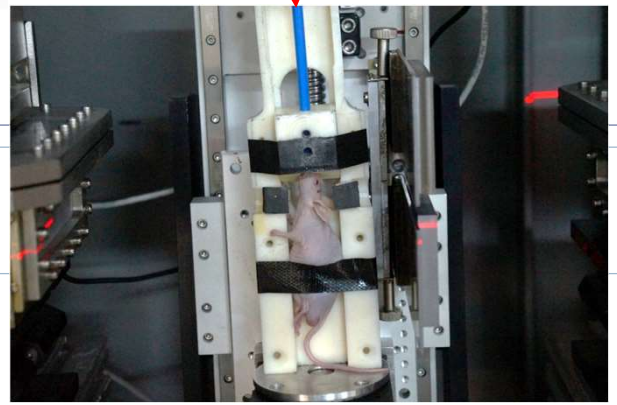

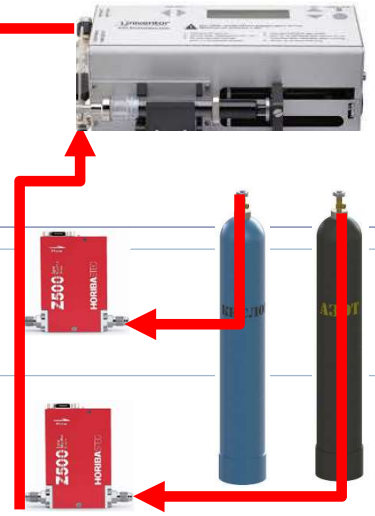

Hipoxia – 95% N2 + 5% O2
Normal atmosphere – 80% N2 + 20% O2
Hyperoxia – 50% N2 + 50% O2

Beamline for study of the fast dynamic processes (detonation, explosion etc.)

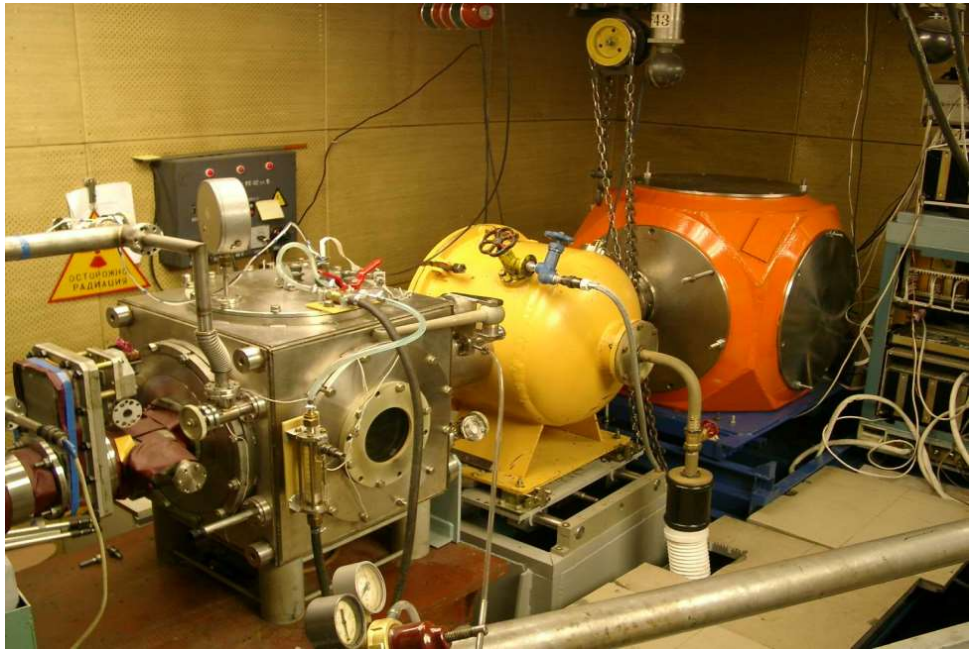

The old submicrosecond process research station of the VEPP-3.

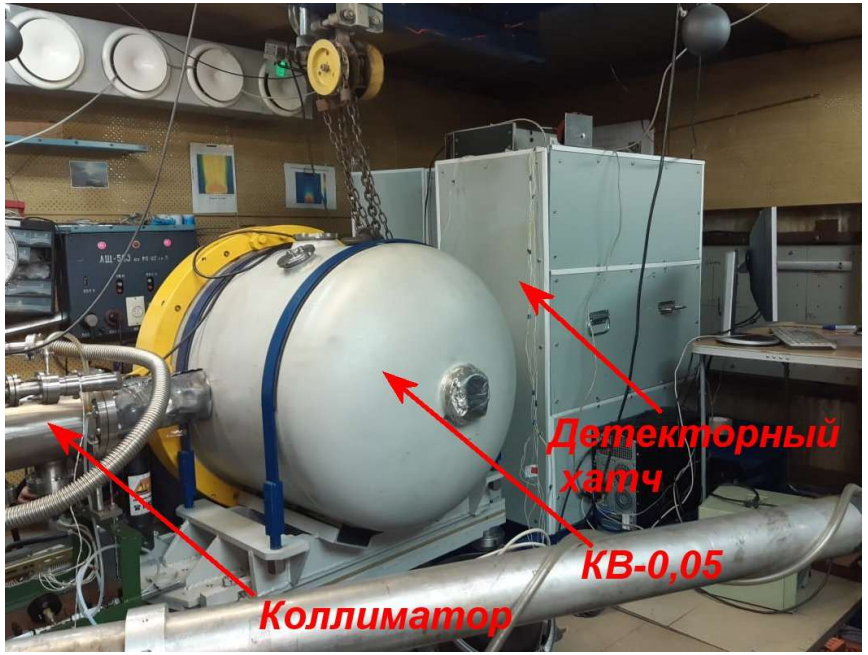

New explosive camera and detector hutch on Channel 0 on VEPP-3.

VEPP-4M Detonation Beamline

Explosive chamber for 250 g TNT

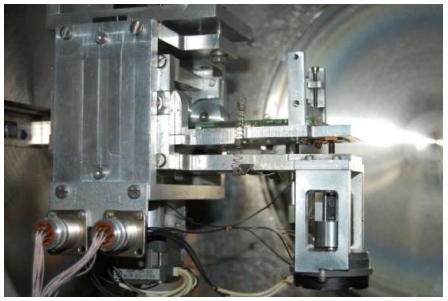

Cratki collimator

Fast detector DIMEX

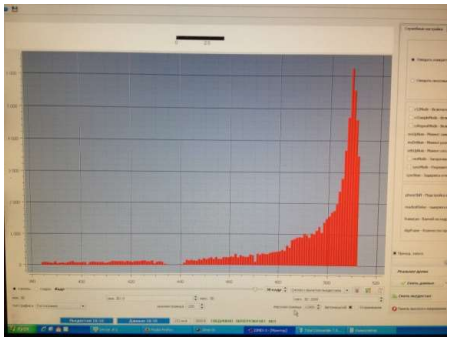

SAX signal from the detonation nanodiamonds

Detonation Diamond nucleation : scale effect

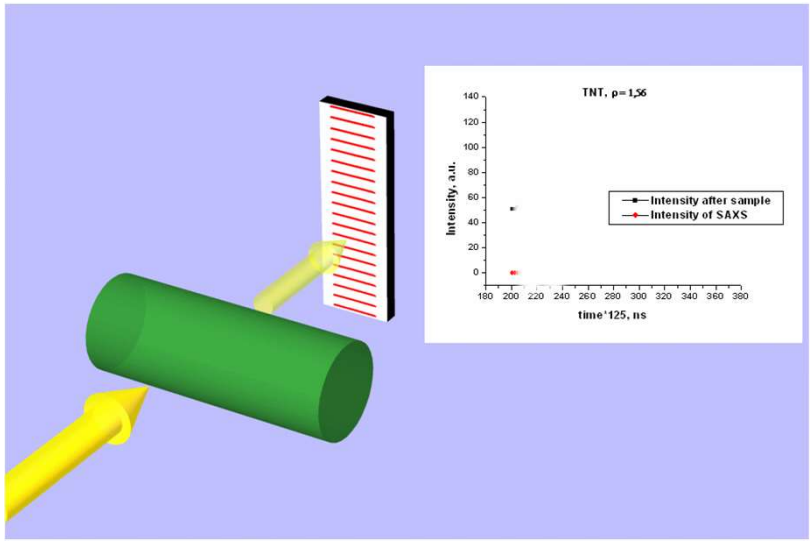

- The scheme of SAXS experiment during detonation of explosive trotyl/hexogen.

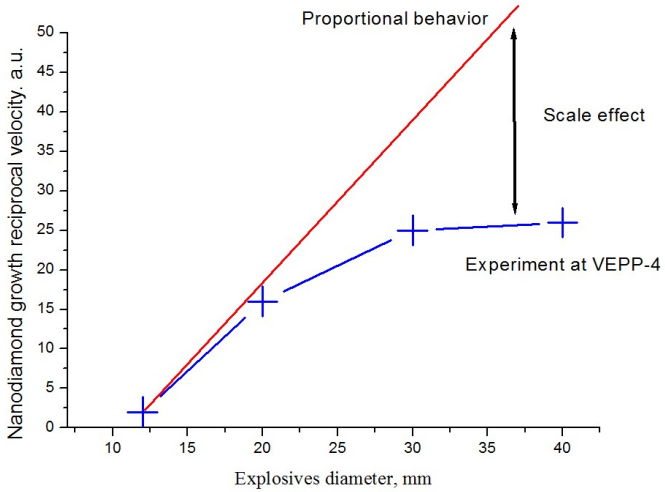

- The scheme of SAXS experiment during detonation of explosive trotyl/hexogen.

- It was found that an increase the mass of explosives leads to increases of produced diamonds mass. Accordingly, increases the rate of formation of diamonds. However, the dependence of the diamonds mass versus the mass of explosive is nonlinear. Also there is non-linear dependence of the formation rate of diamonds versus the weight of the explosives. Thus we observe a scale effect.
- Interpretation: the dependence of chemical reactions from the detonation conditions (diameter), the formation of larger diamonds in the detonation of explosives with large diameters.

Comprehensive study of the dynamics of the dust cloud in gas environments by SR methods, the PDV laser complex and piezosensors.

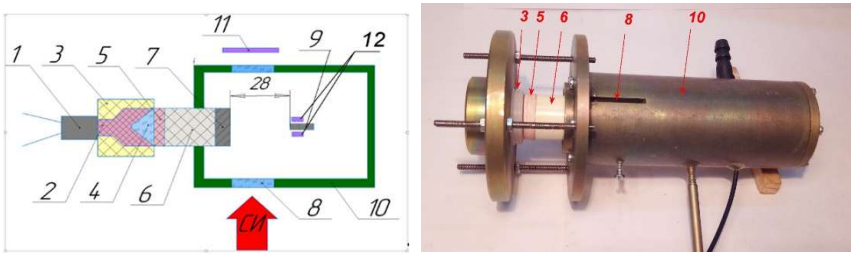

Scheme (left) and general view of experimental assembly: 1-detonator, 3-explosive lens, 6-main charge of THE MB, 7 - tin disk d'26-3 mm; 8 - lavafilm film 0.2 mm thick; 9 - piezo sensor; 10 - hull; 11 - DIMEX detector; 12th PDV collimator

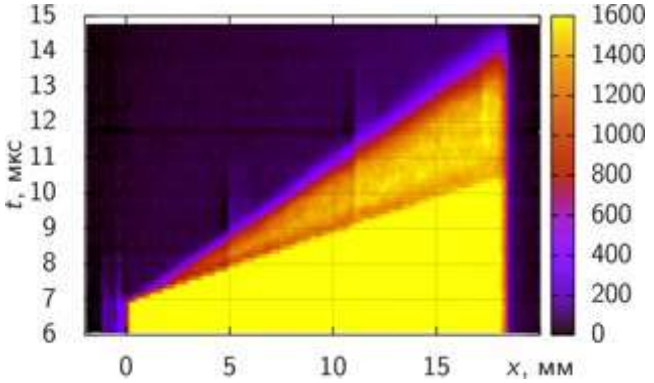

The SR intensity dynamics with 124 ns time steps.

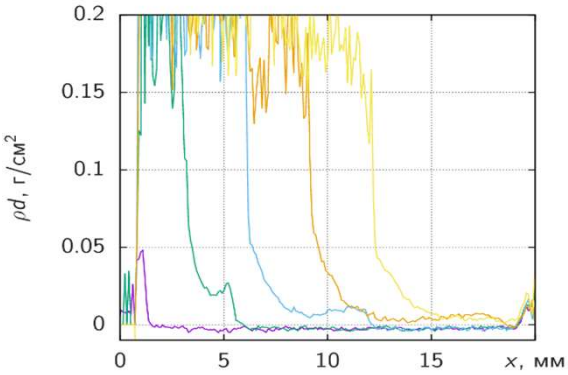

The dynamics of dust mass distributions. Every tenth frame is shown (through 1.24 msec.)

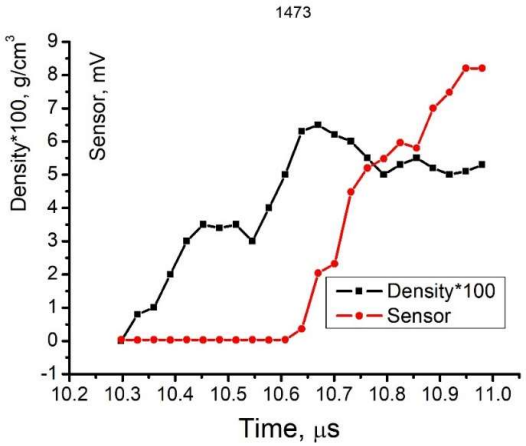

Rz 63

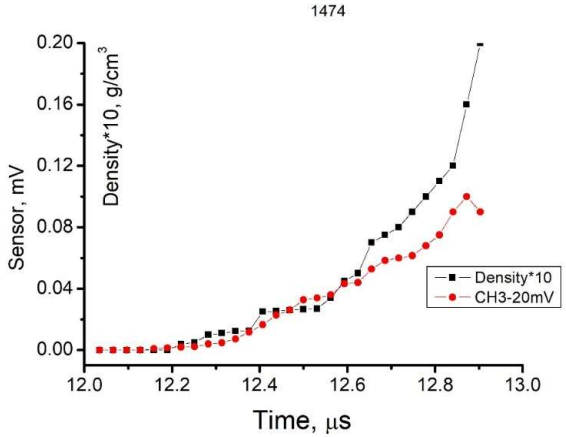

Rz 5

Comparison of piezosensor data with the density of dust flow in the sensor area. With large Rz dust clouds on the SR detector can be seen before the piezosensor registers, readings from the piezosensor (red dots) and the dust flow density recorded by the detector (black dots)

ITER: plasma discharge on the diverter. Material behavior. Model experiment with laser pulse heating

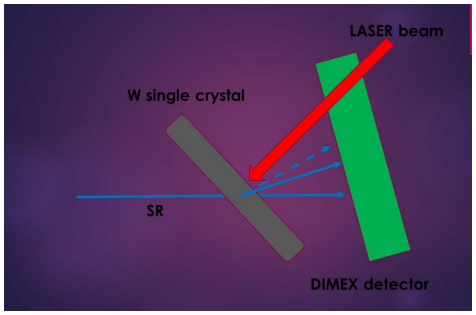

The scheme of model experiment with LASER pulse heating during 100 microseconds.

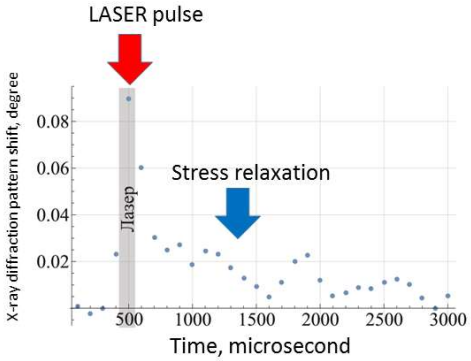

The experimental data of model experiment with LASER pulse heating .

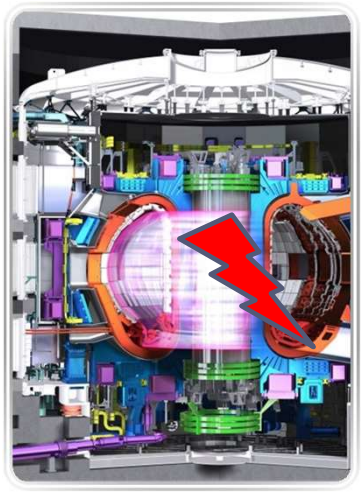

- Now we are preparing an experiment to study the behavior of the crystal lattice of the material of the fusion reactor first wall in a plasma discharge on the diverter

Soft X-ray and VUV metrology station

Optics layout

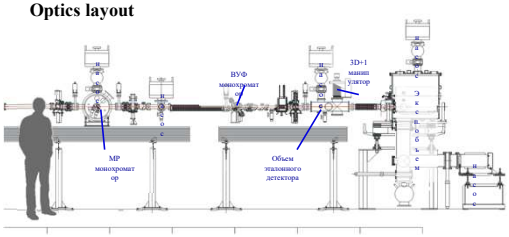

The spectral sensitivity of the reference detector SPD
silicon photodiode development
PTI (St. Petersburg)

The detector is calibrated to the national metrological center German PTB using a cryogenic radiometer. Calibration accuracy - 1%.

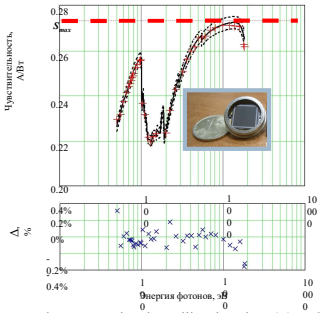

The top graph - the calibration data (+) and approximation of data (solid line) of the model function. The lower graph shows the difference between (x).

The
calorimeter. Absolute detector for absolute measurement of beam powerof 300 mW or more
Measurement accuracy - 2-5%

Two coordinate detector fro Lebedev Institute (Moscow)

Based on CCD E2V tech. (GB)

Gratis monochromator for VUV range

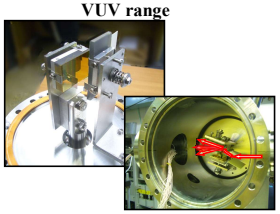

Spectral range: 5 - 100 eV
Spectral resolution: 0.3-2%
The angle of incidence: 70º
Scanning angle: ± 10º
The lattice period: 1/300 mm
Plating: Gold
The fixed position of the output beam in the scanning process - 14 mm

Soft X-ray monochromator

Spectral range: 80-3000 eV
Spectral resolution: 0.1-10%
The range of angles of incidence: 10º- 85º
Mirrors: Y / Mo, Fe / C, W / Si;
Crystals: mica, RbAP, KAP
Adjust the angle of the second mirror: ± 10º
The fixed position of the output beam in the process of scanning the spectrum

Reflectometry system in the experimental volume

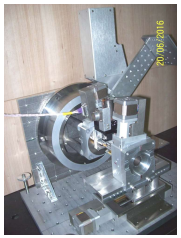

It allows to work with mirrors, crystals and diffraction gratings. Investigation of the reflection coefficients, rocking curves, quality focusing systems, etc.

Sensitivity map measurements

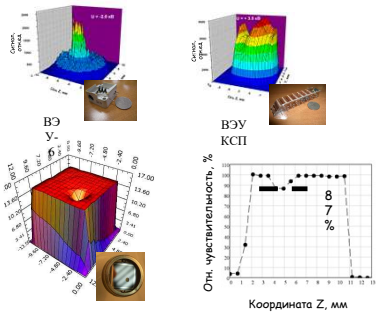

Map sensitivity photodiode FDUK-100UV after local irradiation dose of 1.8 MGrey (123 J / cm2)

Calibration meter solar activity for a geostationary satellite "Electro-L №3" Customer - Institute of Applied Physics (Moscow)

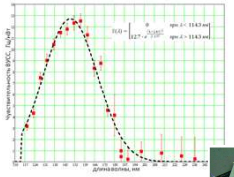

Absolute spectral sencitivity

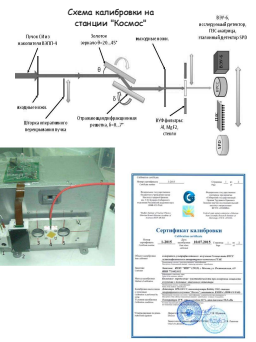

certified measurement procedure

СКИФ

Siberian circular photons source
(SKIF, СКИФ)

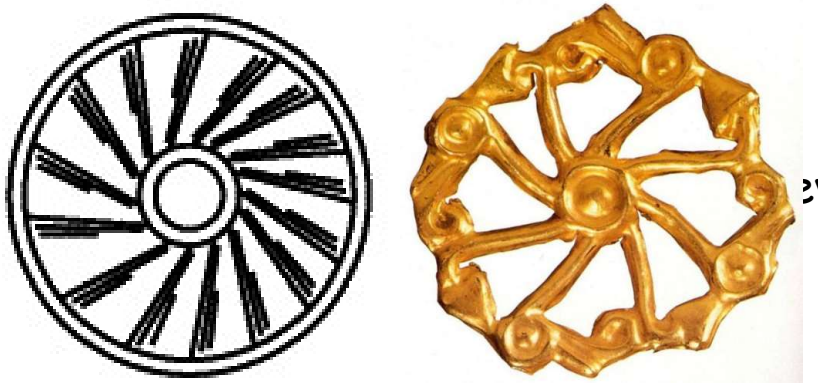

(СКИФ = Scythian)

26

BU1

TECHNOPROM Forum, Novosibirsk, August 28, 2018

Слайд 27

BU1 BINP User; 04.10.2018

Light sources (energy-emittance plot)

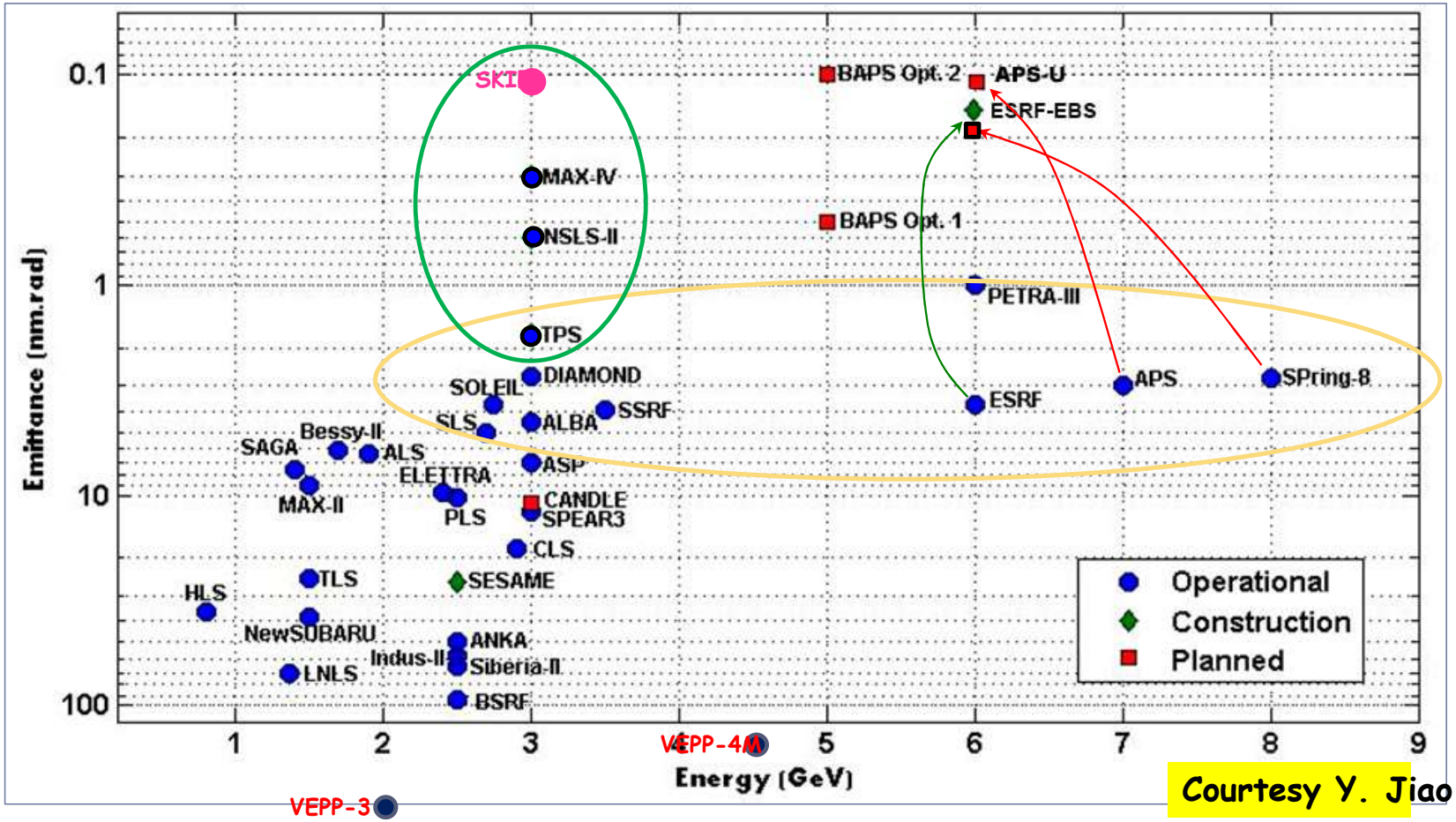

General layout of the SKIF Light Source

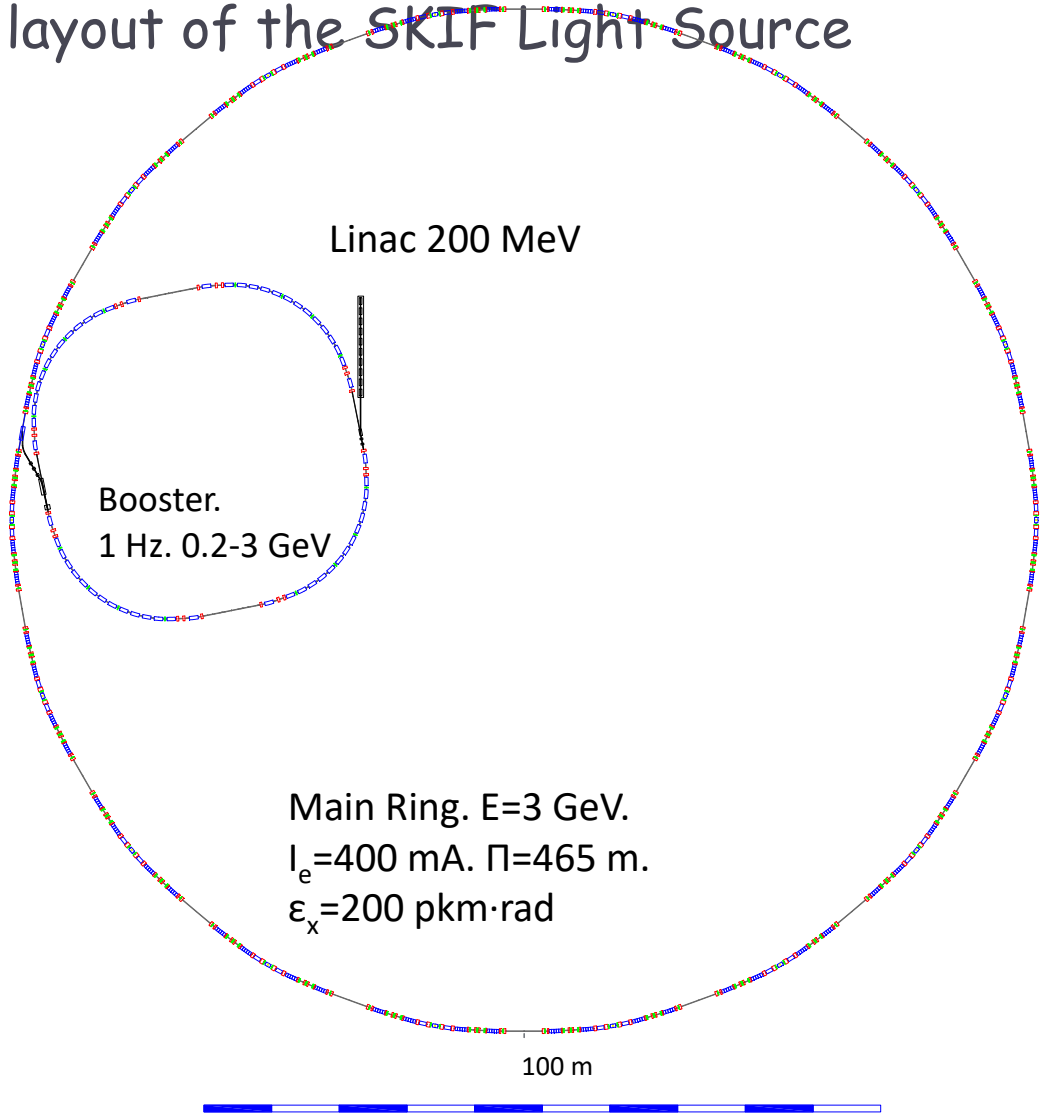

Energy	3 GeV
Beam current	Up 400 mA
Lattice	Mulibend achromat (7 bends in cell)
Symmetry	16 cells
Emittance	75 pkm rad (without ID)
Injection type	Top up
Circumference	~ 480 m
ID	14 wigglers or ondulators
RF	350 MHz + 1050 MHz

SKIF lattice

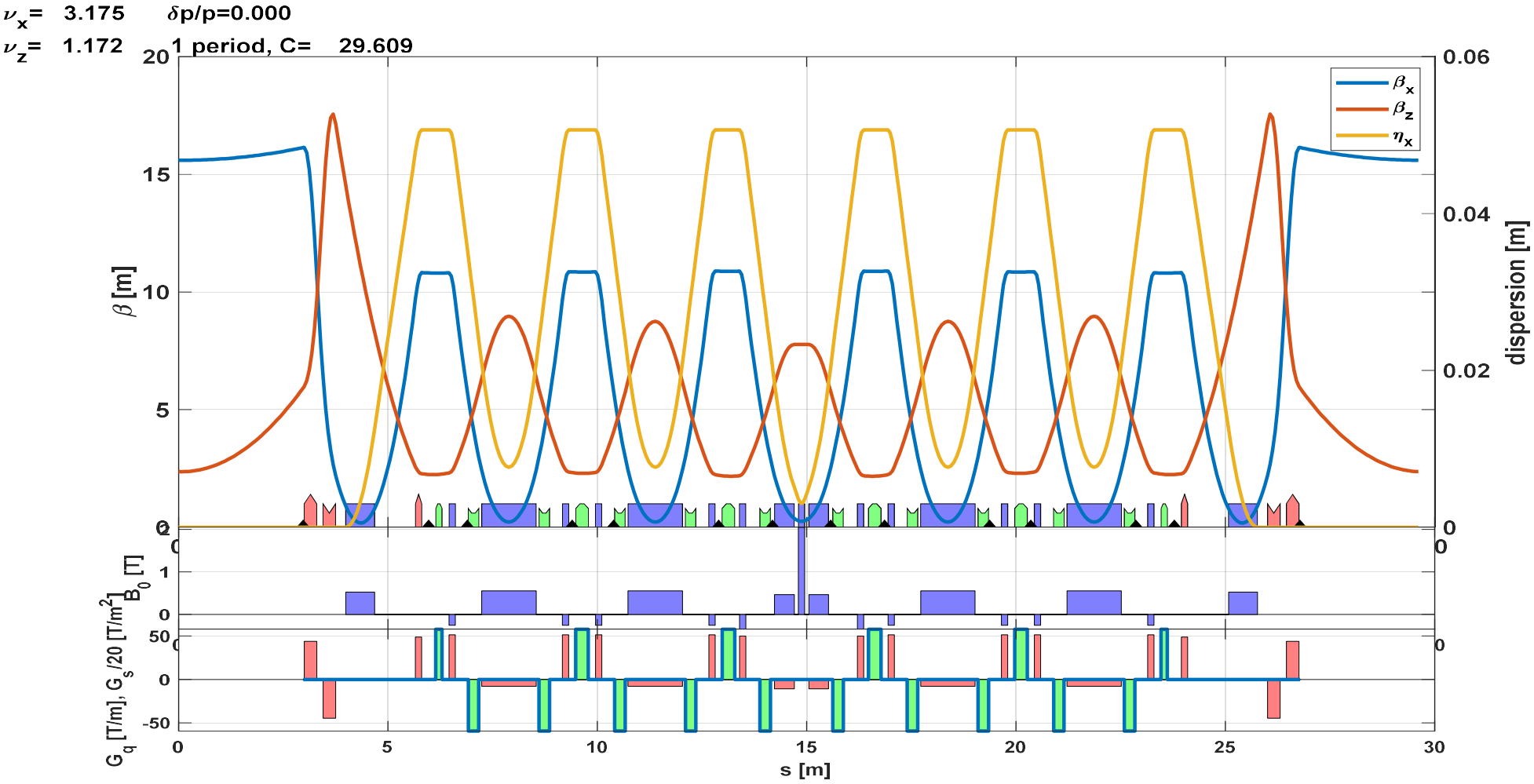

СКИФ

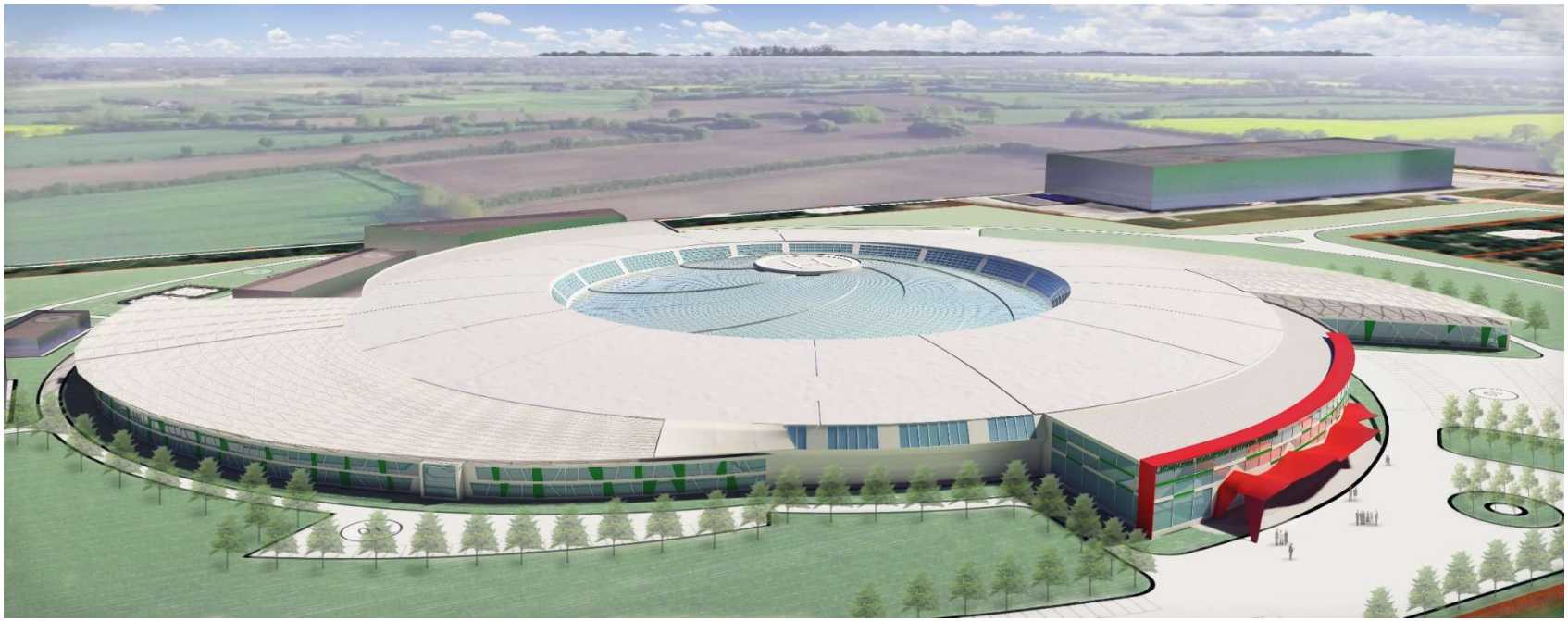

Phase-1 beamlines

- Nanofocus beamline. scanning μXRF (**V.S. Sobolev Institute of Geology and Mineralogy**);
- Structural diagnostic beamline (**Institute of Solid State Chemistry and Mechanochemistry**);
- Fast dynamic processes beamline (**Lavrentyev Institute of Hydrodynamics**);
- XAFS-spectroscopy and MCD beamline (**Boreskov Institute of Catalysis**);
- Phase contrast imaging and microtomography beamline (**Budker Institute of Nuclear Physisc**);
- Soft X-ray spectroscopy and reflectometry beamline (**Nikolaev Institute of Inorganic Chemistry**).

SKIF Light Source for Siberian Region

Main parameters

Parameter	Value
Energy	3 GeV
Number of beamlines	30
Circumference	470 m

Interests

50 institutes of the Siberian. Ural and Far East branches Russian Academy od Sciences	
More than 10 universities	
Industry	Chemical. Energy production. mechanical engineering. pharmacy. microbiological etc

Workplaces

Workplaces	300 (100 – scientific)
Users (every year)	More than 10000

Schedule and cost

Phase	Time	Cost
Phase - 1	5 year	30 billions rubles
Phase - 2	5 лет	2 billions rubles every year

Powerful impact for development industrial and scientific infrastructure of the Siberia region

Critical research directions

+ new materials: Na_2He (>100 GPA). nanodiamonds. catalysts. composite materials

+ new propeties: high temperature (200 K) superconductivity in H_2S 150 GPa

+ new medicine: Vitrinol. target delivery

+ new technologies: synthesis and diagnostics of nano- and hybrid materials. molecular biological processes. modified surfaces

+ future energy production: Comprehensive research of materials for thermonuclear reactors

+ import substitution. lack of analogues in Russia and much. much more ...


Thank you for attention
Институт Ядерной Физики СО РАН